Journal of Marine Science and Technology

Volume 26 | Issue 1 Article 6

# COMPARISONS OF POSITION CONTROL OF VALVE-CONTROLLED AND PUMP-CONTROLLED FOLDING MACHINES

Ray-Hwa Wong
*Department of Mechanical Engineering, Hwa Hsia University of Technology, New Taipei City, Taiwan, R.O.C*,
rhwong@cc.hwh.edu.tw

Wei-Heng Wong
*Department of Electrical Engineering, National Taiwan Ocean University, Keelung, Taiwan, R.O.C.*

# COMPARISONS OF POSITION CONTROL OF VALVE-CONTROLLED AND PUMP-CONTROLLED FOLDING MACHINES

## Acknowledgements

This work is funded by Ministry of Science and Technology of Taiwan, R.O.C. under the grant number MOST 104-2221-E146-010-.

Journal of Marine Science and Technology, Vol. 26, No. 1, pp. 64-72 (2018)
DOI: 10.6119/JMST.2018.02_(1).0008

# COMPARISONS OF POSITION CONTROL OF VALVE-CONTROLLED AND PUMP-CONTROLLED FOLDING MACHINES

Ray-Hwa Wong[1] and Wei-Heng Wong[2]

Key words: valve-controlled, pump-controlled, electro-hydraulic servo control, coupled adaptive self-organizing sliding-mode fuzzy controller.

## ABSTRACT

Control units of electro-hydraulic double-axial folding machine can be classified as throttling type (valve-controlled) and volumetric type (pump-controlled). This paper focuses to compare their control performances. Valve-controlled folding machine (VCFM) has higher supply pressure, different circuit resistance between subsystems. Pump-controlled folding machine (PCFM) has variable working pressure and circuit resistance is slightly different. The folding machine is a coupled system and has significant structural interaction. This paper proposes coupled adaptive self-organizing sliding-mode fuzzy controllers to improve folding machine's level control performance. It found higher supply pressure of VCFM cause faster transient response, larger maximum overshoot via a variety of coupled intensity synchronous level control experiments. Experimental results indicate that their transient and steady state responses are similar, but pump-controlled folding machine has better level control accuracy than valve-controlled folding machine.

## I. INTRODUCTION

Electro-hydraulic servo control systems can be classified as throttling type and volumetric type control systems. The throttling type system is controlled by servo-valve and generally has fast response. But, its noise level is high and energy efficiency is low. In the contrast, the volumetric type system is pump-controlled and has low noise level and high energy efficiency. Nevertheless, its response is sluggish. Until now, major applications of electro-hydraulic servo systems are valve-controlled. However, due to the shortage of energy and the improvement of AC servo motor, the research in pump-controlled system has become more important lately (Chiang, 2011).

In this paper, it focuses to compare the performance of valve-controlled folding machine (VCFM) and pump-controlled folding machine (PCFM) in position control. The electro-hydraulic folding machine is a double-axial actuating system, which is a multiple-input and multiple-output system. Its bending plate induces evident structural interactions, for comparisons, control units of valve-controlled and pump-controlled are designed to have similar working trace in experiments. However, VCFM has higher supply pressure, different circuit resistance between subsystems. Higher supply pressure lead to faster response in transient, different circuit resistance induce worse synchronism of two axes. PCFM has variable working pressure and different circuit resistance, variable working pressure lead to better synchronism especially in transient. By means of synchronous level experiments, this paper compares their control performance.

The electro-hydraulic folding machine is a non-linear control system. Without the detailed model, fuzzy control algorithms have been found to be effective in dealing with non-linear, complicated and ill-defined systems. The sliding-mode controller (Chiang et al., 2009; Kim and Wang, 2009; Zhang et al., 2012; Yuan et al., 2015), self-learning fuzzy controller (Jones et al., 2000; Chiang and Chien, 2003) and adaptive controller (Tar et al., 2005; Cheng and Pan, 2008; Yang et al., 2010; Mohanty and Yao, 2011; Chen, 2015; Mirkin and Gutman, 2015; Yang et al., 2016) have been widely applied for electro-hydraulic control systems. To integrate the sliding-mode, self-learning fuzzy rules and adaptive control law, this paper proposes the coupled adaptive self-organizing sliding-mode fuzzy controller (CASOSMFC) for the synchronous level control of VCFM and PCFM. The sliding surface function is used to reduce two-dimensional system variables into one-dimensional system variables. The one-dimensional self-learning mechanism provides optimized fuzzy rules online. The adaptive control law is used to adjust defuzzification scaling factors on-line.

This paper will analyze time response of transient and steady state of different coupling intensity in PCFM and VCFM and see if PCFM is an option to replace VCFM in the synchronous level control applications, to improve energy issues.

*Paper submitted 06/25/16; revised 01/20/17; accepted 09/04/17. Author for correspondence: Ray-Hwa Wong (e-mail: rhwong@cc.hwh.edu.tw).*
*[1] Department of Mechanical Engineering, Hwa Hsia University of Technology, New Taipei City, Taiwan, R.O.C.*
*[2] Department of Electrical Engineering, National Taiwan Ocean University, Keelung, Taiwan, R.O.C.*

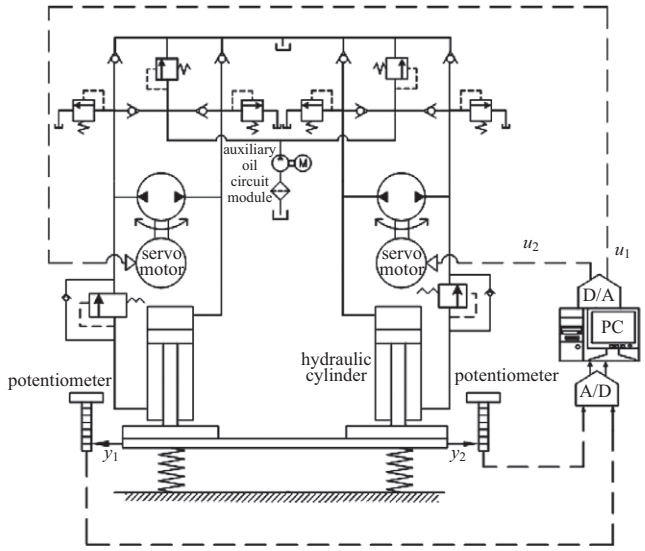


**Fig. 1. Schematic diagram of a double-axial hydraulic pump-controlled folding machine.**

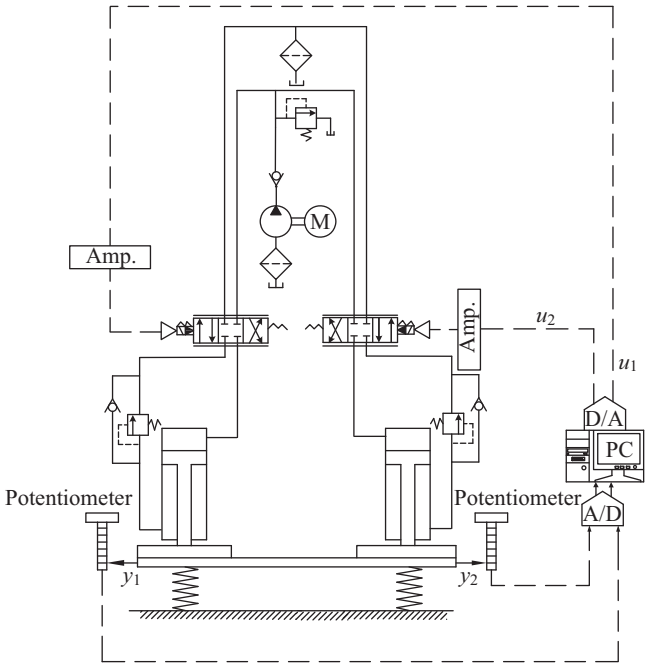


**Fig. 2. Schematic diagram of a double-axial hydraulic valve-controlled folding machine.**

## II. SYSTEM DESCRIPTIONS

The schematic diagram of a double-axial PCFM is shown as Fig. 1. Its synchronous folding process is required in metal forming and folding applications. It contains two hydraulic pump-controlled servo actuating sub-systems, a heavy folding plate and elastic loading. Hydraulic circuit resistance of two sub-systems is almost the same.

The inside diameter of actuator is 105 mm, and the rod diameter is 95 mm. The distance between actuators is 500 mm. The hydraulic power unit contains two sets of 12 ml/rev fixed displacement pump, which are driven by 2.0 KW AC servo motors, the revolution of servo motor is variable. Positions are measured by potentiometers. The mass of the folding plate is 214 kg. Two elastic springs are used to simulate the workpiece's behavior of the folding process. The distance between elastic springs is adjustable to simulate the different coupled intensity. The resolution of A/D and D/A converter are 12 bits. The personal computer is a Core i5 microcomputer system. The control program is developed by C Language.

Hydraulic circuit resistance of PCFM of two sub-systems is slightly different and its synchronism is better.

The schematic diagram of VCFM is shown in Fig. 2. The structure of VCFM is the same as PCFM. The hydraulic power unit contains two sets of 40 l/min servo valve and a hydraulic pump which is driven by a 3.7 KW AC induction motor. Owing to the difference of circuit resistance and interference between two sub-systems, VCFM is difficult to achieve the synchronous level function.

## III. CONTROL SCHEME

The folding machine is a coupled multiple-input and multiple-output control system. The block diagram of proposed CASOSMFC

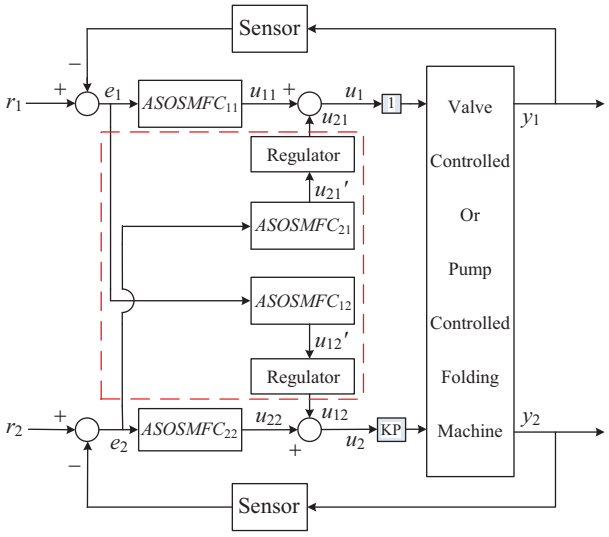


**Fig. 3. Block diagram of control structure.**

control structure is shown as Fig. 3.

The detail of ASOSMFC is shown as Fig. 4. In general, the fuzzy logic control is developed by two system variables ($e$, $ce$) and two-dimensional fuzzy rules. Sliding-mode fuzzy controller is to simplify fuzzy variables to one-dimension and reduce fuzzy rules. The fuzzy sliding surface is shown in Fig. 5. It is described as

$$s = ce + \alpha e \tag{1}$$

Here $e$ is error between command and output, $s$ is called the slid-

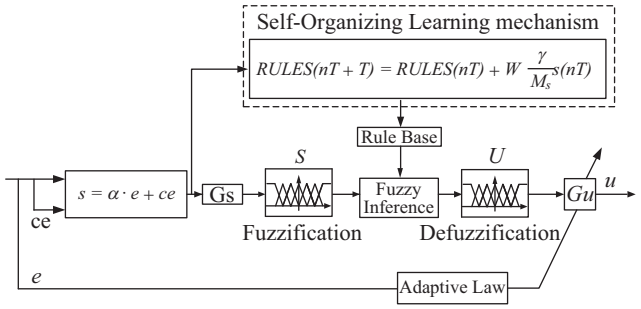


**Fig. 4. Configuration of adaptive self-organizing sliding-mode fuzzy controller.**

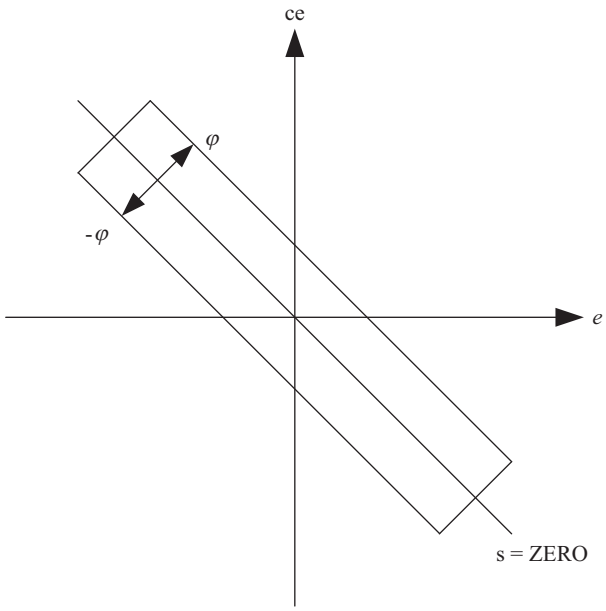


**Fig. 5. The fuzzy sliding surface.**

ing variable. $\alpha$ is a positive constant which represents the slope of the fuzzy sliding surface $s$ = ZERO and $\varphi$ is the boundary layer width of the sliding surface $s$. The sliding surface can be divided into 13 sections by the triangular membership function sets of M( $\tilde{s}$ ) = {NVB, NB, NM, NSM, NS, NVS, ZO, PVS, PS, PSM, PM, PB, PVB}. The membership function sets of the control voltage $u$ is defined as M( $\tilde{u}$ ) = {NVB, NB, NM, NSM, NS, NVS, ZO, PVS, PS, PSM, PM, PB, PVB}. Proportional factor $G_s$ and $G_u$ are used to normalize between system variables and the universal of fuzzy sets. The fuzzy inference is based on the Max-Min product composition and is used to operate fuzzy control rules. The height method (Maldonado et al., 2014) is used to defuzzify fuzzy sets to attain the control signal.

The two-dimensional fuzzy rule learning mechanism (Lin and Lian, 2008) is

$$\Delta u(nT) = \frac{\gamma}{M}\left[(1-\zeta)\cdot e(nT) + \zeta \cdot ce(nT)\right] \tag{2}$$

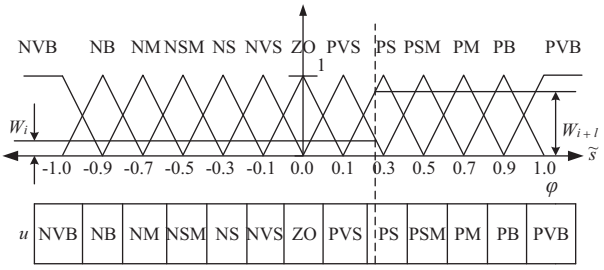


**Fig. 6. Membership function of S and rule base.**

In here, $\Delta u$ is the control voltage correction, $\gamma$ is a weighting factor of learning rate. M is the system gain and $\zeta$ is the weighting factor of control voltage correction. Then, the relationship between $\zeta$ and $\alpha$ is defined as

$$\zeta = \frac{1}{(1+\alpha)},\ \alpha \ge 0,\ 0 \le \zeta \le 1 \tag{3}$$

Substitute Eqs. (3) and (1) into Eq. (2) and then Eq. (2) becomes

$$\Delta u(nT) = \frac{\gamma}{M_s}\left[s(nT)\right] \tag{4}$$

Here $M_s = M(1 + \alpha)$ is a ratio to simulate the relationship between servo amplifier's input and displacement output.

Since each output state in the universe is excited by two modules as shown in Fig. 6.

The correction of each fuzzy rule is modified by its excitation intensity $W$ obtained by the linear interpolation technique. The control voltage $u_i$ of the $i$th rule is

$$u_i(nT+T) = u_i(nT) + W_i\Delta u = u_i(nT) + W_i\frac{\gamma}{M_s}s(nT) \tag{5}$$

According to the linguistic approach, the rule base of self-organizing learning mechanism can be modified as

$$RULES(nT+T) = RULES(nT) + W\frac{\gamma}{M_s}\cdot s(nT) \tag{6}$$

Adaptive law to adjust the defuzzification proportional factor $G_u$, which promote the time response. The quadratic performance index of adaptive law is defined as:

$$J = \frac{1}{2}e^2 \tag{7}$$

The gradient descent algorithm has the advantage of less memory requirement, and it is used to minimize $J$ as

$$\dot{G}_u = -\delta\frac{\partial J}{\partial G_u} = -\delta\cdot e\frac{\partial e}{\partial G_u},\ \delta > 0 \tag{8}$$

$\delta$ is the adaptation gain.

The simplified model between error (e) and output (y) is

$$y = e \cdot K \cdot G_u \cdot M_p$$
$$e = r_d - y = r_d - e \cdot K \cdot G_u \cdot M_p$$
$$e\left(1 + K \cdot G_u \cdot M_p\right) = r_d$$
$$e = \frac{1}{1 + KG_u M_p} r_d$$
$$e = r_d - y = \frac{1}{1 + KG_u M_p} r_d \tag{9}$$

Then, the system model is

$$y = \frac{KG_u M_p}{1 + KG_u M_p} r_d \tag{10}$$

Here $K$ is a fuzzy gain which is the relationship between $e$ and $U$. $M_p$ is plant, $r_d$ represents $r_1$ or $r_1$.

Substitute Eq. (10) into Eq. (9) to obtain

$$\dot{G}_u = \delta \cdot e \cdot r_d \cdot K \cdot M_p \left(1 + KG_u M_p\right)^{-2} \tag{11}$$

Using the backward difference approach, Eq. (11) is indicated in the discrete form as

$$G_u\left(nT + T\right) = G_u\left(nT\right) + \delta \cdot e\left(nT\right) r_d K\left(nT\right) M_p \left(1 + K\left(nT\right) G_u\left(nT\right) M_p\right)^{-2} T \tag{12}$$

Coupled terms of proposed CASOSMFC are indicated in the dashed line of Fig. 3.

If there are not regulators, then $u_1 = u_{11} + u_{21}'$ and $u_2 = u_{22} + u_{12}'$, here the value of $u_{21}'$ is determined by the value of $e_2$. If $e_1 > e_2 > 0$, $e_1$ must be reduced to improve the synchronization performance between $e_1$ and $e_2$. Because $u_{21}'$ is positive, $u_1$ will increase, synchronization between $y_1$ and $y_2$ becomes better. However, $u_{12}'$ is positive, too. It makes $u_2$ increase caused worse synchrony between $y_1$ and $y_2$. If $e_2 < e_1 < 0$, $e_2$ must be increased to improve the synchronization performance between $e_1$ and $e_2$. Since $u_{12}'$ is negative, $u_2$ will reduce, synchronization between $y_1$ and $y_2$ will improve. Meanwhile, $u_{21}'$ is negative, too. It makes $u_1$ reduction caused synchronization worse between $y_1$ and $y_2$. If $e_1 > e_2$, $e_1 \cdot e_2 < 0$, $e_2$ must increase, $e_1$ must be reduced to improve the synchronization performance between $e_1$ and $e_2$. Because $u_{21}'$ is negative, $u_1$ will reduce, synchronization will deteriorate between $y_1$ and $y_2$. Meanwhile, $u_{12}'$ is positive, $u_2$ will increase, it also reduces synchronization between $y_1$ and $y_2$. So, it needs to install two regulators behind $u_{12}'$ and $u_{21}'$, making $u_1 = u_{11} + u_{21}$ and $u_2 = u_{22} + u_{12}$.

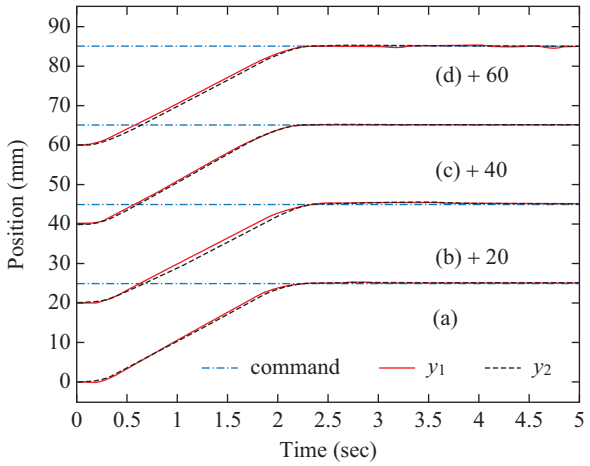


**Fig. 7. Time response of decoupled system and coupled system with variety of $\delta_{ij}$. (a): decoupled, (b): $\delta_{ij}$ = 0.012 without regulator, (c): $\delta_{ij}$ = 0.012, (d): $\delta_{ij}$ = 1.2 in PCFM**

When $e_1 > e_2 > 0$, let $u_1 = u_{11} + u_{21}$, $u_2 = u_{22}$, it can improve synchronization between $y_1$ and $y_2$. In circumstances of $e_2 < e_1 < 0$, $y_1$ and $y_2$ are higher than the step command, and $y_2$ is higher than $y_1$, then the design concept of the regulator is similar to $e_1 > e_2 > 0$, so the control voltage for the two axes are $u_1 = u_{11}$ and $u_2 = u_{22} + u_{12}$.

In the case of $e_1 > e_2 >$ and $e_1 \cdot e_2 < 0$, $y_1$ and $y_2$ are in the opposite sides of step command. In this case, the regulator is designed as $u_1 = u_{11} - u_{21}$ and $u_2 = u_{22} - u_{12}$ to improve the synchronization.

From aforementioned analysis, in order to make the system in better synchronization, the design of regulators are summarized as follows:

For $i = 1, 2\ j = 1, 2$

$$\begin{aligned} &\text{If } e_i > e_j > 0\ i \neq j \text{ then } u_i = u_{ii} + u_{ji}, u_j = u_{jj} \\ &\quad e_i < e_j > 0\ i \neq j \qquad u_i = u_{ii} + u_{ji}, u_j = u_{jj} \\ &\quad e_i \cdot e_j > 0\ i \neq j \qquad u_i = u_{ii} - u_{ji}, u_j = u_{jj} - u_{ij} \\ &\text{else} \qquad\qquad\qquad u_i = u_{ii} \end{aligned} \tag{13}$$

Coupled controllers and regulators are integrated to become a coupled terms as indicated in Fig. 3. Coupled adaptation gain $\delta_{ij}$, $j = 1, 2$, $i \neq j$ are used to adjust $G_{uij}$ in ASOSMFC$_{ij}$. For PCFM learning rate $\gamma_{ij}$ in ASOSMFC$_{ij}$ is chosen by try and error as 0.006.

Fig. 7 is time response of $\delta_{ij} = 0$ (decoupled control system),

$\delta_{ij} = 0.012$ with and without regulators, and $\delta_{ij} = 1.2$. It shows that time response of $\delta_{ij} = 0.012$ with regulators has better synchronism in transient and steady state than the decoupled control system, because $\delta_{ij}$ can adjust defuzzification proportional factors to enhance coupled control voltage and to improve synchronous performance. $\delta_{ij} = 0.012$ without regulators cannot determine proper $u_{12}'$ and $u_{21}'$ to achieve the synchronous function and causes the worst synchronism in the transient process comparing with decoupled control system and other coupled control system. Coupled control system with $\delta_{ij} = 1.2$ has excessive amend control voltage, induce significant oscillations and degrade the synchronous performance in the steady state. From the previous studies, regulators are required in the coupled control system, and the coupled adaptation gain $\delta_{ij}$ of adaptive law will be appropriately chosen as 0.012 for PCFM. VCFM has the similar effects of the coupled terms.

## IV. SETTING THE SAME BASIS OF PCFM AND VCFM

PCFM uses two groups of the power unit to drive two subsystems, the resistance of two subsystems is almost the same, its synchronicity is better, the saturation voltage of two axes of PCFM is the same.

VCFM uses a group of the power unit to drive two subsystems, the resistance of two subsystems is different, resulting in the synchronization difference. Therefore, the proportional gain of two subsystems must be adjusted before the experiment, and set up different saturation voltage for the two subsystems, which is to establish the two sub-systems of VCFM have the same conditions and has the same basis as PCFM.

Setting the same basis of PCFM and VCFM as follows:

1. Using SMFC in PCFM to find the output response.
2. Using P-control in PCFM, by trial and error to make the transient slope of P-control and SMFC in PCFM are very close, suppose the proportion gain of P-control of two axes are $K_1$ and $K_2$, then $\frac{K_2}{K_1}$ is the proportional gain ratio KP of PCFM in Fig. 3.
3. Using P-control in VCFM, by trial and error to make the transient slope of P-control and P-control in PCFM are very close, then records the saturation voltage of two axes of VCFM, suppose the proportion gain of P-control of two axes are $K_1$ and $K_2$, then $\frac{K_2}{K_1}$ is the proportional gain ratio KP of VCFM in Fig. 3.

VCFM and PCFM have the same basis at this moment, in the same basis, output response of P-control of VCFM is shown in Fig. 8. Because the output voltage is proportional to the error in the P-control, namely $u = Ke$, at saturation voltage, $u_{sat} = Ke_{sat}$, here, $u_{sat}$ is the saturation voltage, $e_{sat}$ is the saturation error, the saturation voltage of two subsystems of P-control is different in VCFM, but the saturation errors of two subsystems are the same, as shown in Fig. 9.

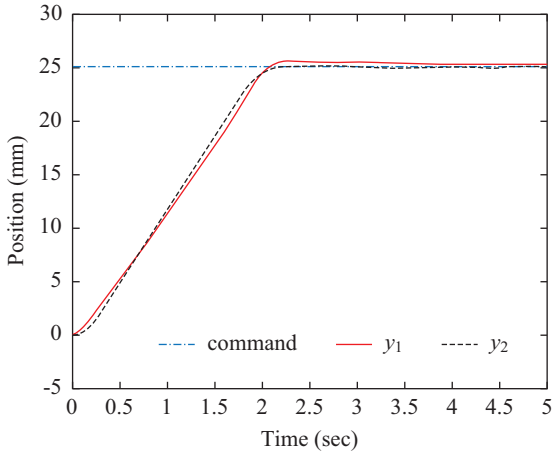


**Fig. 8. Output response of P-control of VCFM.**

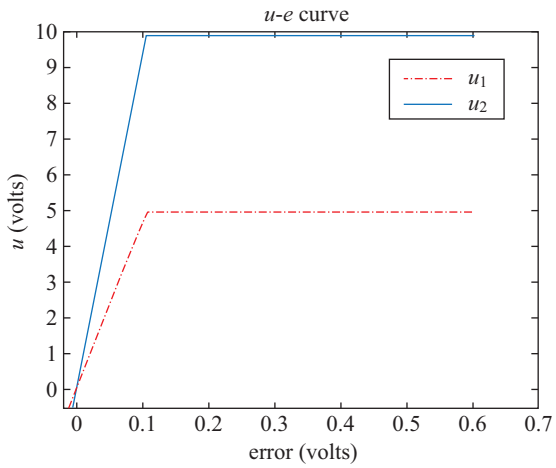


**Fig. 9. u-e diagram of P-control of VCFM.**

## V. EXPERIMENTAL RESULTS

In this paper, level control experiments of VCFM and PCFM are used to compare their characteristics. Owing to unsymmetrical characteristics of VCFM, the saturation voltages of left and right axes are significantly different in the level control process. However, PCFM has less systems' asymmetry and saturation voltages of both axes are the same.

In experiments, parameters of VCFM and PCFM are properly chosen as $\alpha_{11} = \alpha_{22} \neq \alpha_{12} = \alpha_{21} = 1$, $G_{s11} = G_{s22} = 1.67$ and $M_s = 1$, theirs command are step function. The sampling time is $T = 0.01$ seconds. Initial fuzzy rules are (-1, -0.9, -0.7, -0.5, -0.3, -0.1, 0, 0.1, 0.3, 0.5, 0.7, 0.9, 1)

Let the error of left axis is $e_1(nT)$, the error of right axis is $e_2(nT)$, the synchronous error is defined as

**Table 1. Parameters of VCFM and PCFM.**

| | $G_{uii}$ | $G_{uij}$ | $\gamma_{ii}$ | $\gamma_{ij}$ | $\delta_{ii}$ | $\delta_{ij}$ |
|---|---|---|---|---|---|---|
| VCFM | On line adjustment $G_{uii}$ (0) = 28 | On line adjustment $G_{uij}$ (0) = 0 | 0.006 | 0.006 | 4 | 0.02 |
| PCFM | On line adjustment $G_{uii}$ (0) =12 | On line adjustment $G_{uij}$ (0) = 0 | 0.006 | 0.006 | 22 | 0.012 |

**Table 2. PCFM fuzzy rules table of $\gamma$= 0~0.6 at $t$ = 5 s.**

| | NVB | NB | NM | NSM | NS | NVS | ZO |
|---|---|---|---|---|---|---|---|
| $\gamma = 0$ | -1 | -0.9 | -0.7 | -0.5 | -0.3 | -0.1 | 0 |
| $\gamma = 0.006, y_1$ | -1 | -0.9 | -0.7 | -0.5 | -0.3 | -0.1004 | 0.0014 |
| $\gamma = 0.006, y_2$ | -1 | -0.9 | -0.7 | -0.5 | -0.3 | -0.1005 | 0.0006 |
| $\gamma = 0.06, y_1$ | -1 | -0.9 | -0.7 | -0.5 | -0.3 | -0.114 | -0.0084 |
| $\gamma = 0.06, y_2$ | -1 | -0.9 | -0.7 | -0.5 | -0.3 | -0.1176 | -0.0061 |
| $\gamma = 0.6, y_1$ | -1 | -0.9 | -0.7 | -0.5 | -0.3 | -0.5976 | 0.1182 |
| $\gamma = 0.6, y_2$ | -1 | -0.9 | -0.7 | -0.5 | -0.3 | -0.1 | 0.2522 |
| | PVS | PS | PSM | PM | PB | PVB | |
| $\gamma = 0$ | 0.1 | 0.3 | 0.5 | 0.7 | 0.9 | 1 | |
| $\gamma = 0.006, y_1$ | 0.1351 | 0.3846 | 0.6328 | 0.8884 | 1 | 1 | |
| $\gamma = 0.006, y_2$ | 0.1332 | 0.3829 | 0.6392 | 0. 9069 | 1 | 1 | |
| $\gamma = 0.06, y_1$ | 0.382 | 1 | 1 | 1 | 1 | 1 | |
| $\gamma = 0.06, y_2$ | 0.3787 | 1 | 1 | 1 | 1 | 1 | |
| $\gamma = 0.6, y_1$ | 1 | 1 | 1 | 1 | 1 | 1 | |
| $\gamma = 0.6, y_2$ | 1 | 1 | 1 | 1 | 1 | 1 | |

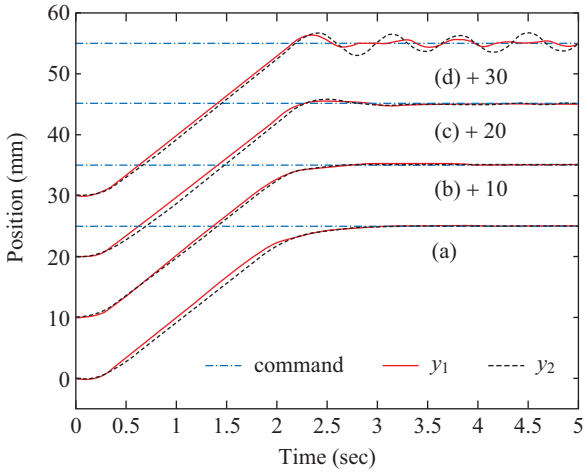


**Fig. 10. ime response of variety $\gamma$: (a): $\gamma$= 0, (b): $\gamma$= 0.006, (c): $\gamma$= 0.06, (d): $\gamma$= 0.6 in PCFM.**

$$\bar{e}(nT) = \left| e_1(nT) - e_2(nT) \right| \tag{14}$$

The average synchronous error is then defined as

$$\bar{e}_{av} = \frac{\sum_{n=1}^{N} \left| \bar{e}(nT) \right|}{N} \tag{15}$$

In addition, $\bar{e}_{SS}$ is the steady state synchronous error.

Learning rate $\gamma$, adaptation gain $\delta_{ii}$ and coupled adaptation gain $\delta_{ij}$ are properly chosen to setup CASOSMFC of VCFM and PCFM as shown in Table 1.

Taking the PCFM as an example, Fig. 10 shows time responses of $\gamma$= 0, 0.006, 0.06 and 0.6 of folding process. $\gamma$= 0 means the fuzzy rules table being fixed and it can't overcome the system uncertainties and coupling effects properly. For $\gamma$> 0, it can adjust fuzzy rules table online and has better tracking and synchronous level control performance than $\gamma$ = 0. To compare their performance, $\gamma$= 0.006 has better synchronous performance and tracking error than those of $\gamma$= 0.06. $\gamma$= 0.06 has oscillation in steady state. $\gamma$= 0.6 has the worst level control performance in the steady state. Its' oscillation is evidently.

Table 2 shows the steady state rules table of PCFM when $\gamma$= 0~0.6 at $t$ = 5 sec. As $\gamma$ increases, the value in the corresponding fuzzy rules table will increase, so some values will reach the limit, resulting in oscillation in Fig. 10.

Overshoot of step response is not obvious in PCFM, so the error $e = r_d - y$ changes from about 25 mm to 0 mm. The error change $ce$ compare with the error e are relatively small. When the sliding variable $s = \alpha e + ce$ is multiplied by the fuzzification proportional factor, its value is always positive, and then mapped to the fuzzy rule membership function from the NVS to the PVB, since the fuzzy rule from NVB to NS are negative, so the fuzzy rule from NVB to NS has not changed.

In experiments, various loading springs to simulate different working pieces indicates variety coupled intensity. Experimental results are used to evaluate and compare performances of VCFM and PCFM. Case 1 has symmetric loading which springs are

**Table 3. Performance indices of different cases (unit: mm).**

| | | Rising time (sec) | | Delay time (sec) | Peak time (sec) | Max. oveshoot (%) | $\overline{e}_{av}$ (mm) | $\overline{e}_{SS}$ (mm) |
|---|---|---|---|---|---|---|---|---|
| Case 1 | VCFM | $y_1$ | 2.11 | 1.05 | 2.31 | 2.07 | 0.25 | 0.03 |
| | | $y_2$ | 2.09 | 1.11 | 2.28 | 1.61 | | |
| | PCFM | $y_1$ | 2.40 | 1.13 | 2.93 | 0.77 | 0.14 | 0.06 |
| | | $y_2$ | 2.23 | 1.15 | 2.55 | 1.16 | | |
| Case 2 | VCFM | $y_1$ | 2.07 | 1.05 | 2.31 | 1.40 | 0.26 | 0.04 |
| | | $y_2$ | 2.10 | 1.10 | 2.43 | 1.44 | | |
| | PCFM | $y_1$ | 2.26 | 1.12 | 2.44 | 0.93 | 0.16 | 0.06 |
| | | $y_2$ | 2.20 | 1.13 | 2.62 | 1.39 | | |
| Case 3 | VCFM | $y_1$ | 2.09 | 1.06 | 2.26 | 1.99 | 0.29 | 0.05 |
| | | $y_2$ | 2.10 | 1.13 | 2.72 | 1.66 | | |
| | PCFM | $y_1$ | 2.48 | 1.10 | 3.24 | 0.62 | 0.19 | 0.07 |
| | | $y_2$ | 2.38 | 1.15 | 3.34 | 0.65 | | |

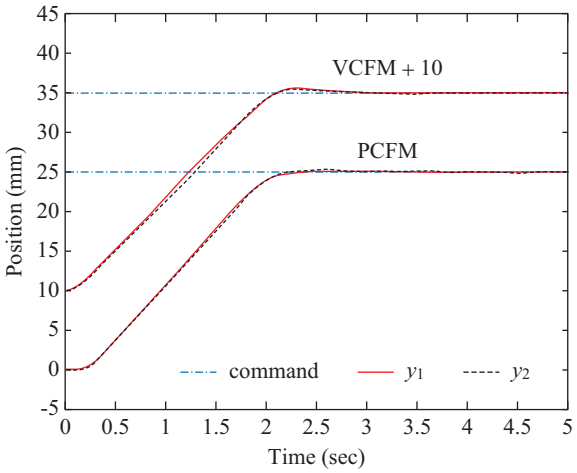


**Fig. 11. Step response of PCFM and VCFM of Case 1.**

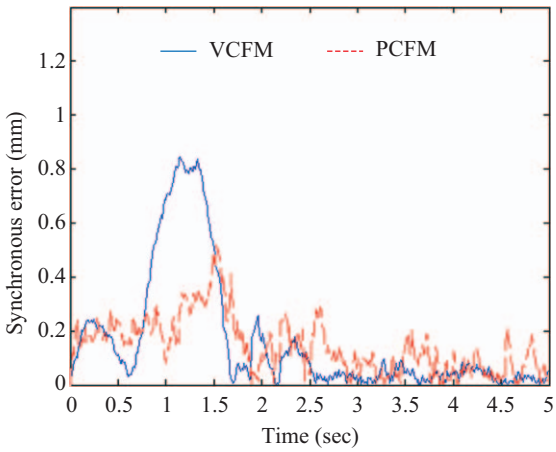


**Fig. 12. $\overline{e}$ of Case 1 of step command.**

directly installed beneath actuators. The loading ratio of two actuators is 1:1. Case 2 is a medium unsymmetrical loading case. The right loading spring is shifted to the left and the distance between two loading springs is 305 mm. The loading ratio is 2.3:1. Next, Case 3 is a large unsymmetrical loading and large coupled intensity case. The right spring is shifted to the left further and the loading ratio is 4.6:1.

Fig. 11 is the step response of VCFM and PCFM of Case 1. Fig. 12 is their synchronous error $\overline{e}$. Supply pressure of VCFM is higher and maintains at constant, causing its transient response faster than PCFM, because its faster transient response than PCFM, and it uses a group of the power unit to drive two subsystems, the resistance of two subsystems is different, resulting in its synchronicity worse than PCFM. Therefore, the rising time, delay time and the peak time of VCFM is shorter, its maximum overshot is larger and it has worse $\overline{e}_{av}$. The initial supply pressure of PCFM is 10 kgf/cm$^2$. The working pressure during the process is variable. Its $\overline{e}_{av}$ are better, rising time, delay time, peak time are longer, the maximum overshoot is small. Their performance indices are summarized in Table 3. It indicates that the rising time of $y_1$ and $y_2$ are 2.11 s and 2.09 s which are shorter than 2.40 s and 2.23 s of PCFM. The delay time of VCFM is 1.05 s and 1.11 s which are shorter than 1.13 s and 1.15 s of PCFM. Similarly, the peak time of VCFM is 2.31 s and 2.28 s which are shorter than 2.93 s and 2.55 s of PCFM. However, the maximum overshoot of $y_1$ and $y_2$ of VCFM are 2.07% and 1.61%, which are greater than 0.77% and 1.16% of PCFM. $\overline{e}_{av}$ of VCFM is 0.25 mm, it is worse than 0.14 mm of PCFM. However, $\overline{e}_{SS}$ of VCFM is 0.03 mm, which is better than 0.06 mm of PCFM.

Fig. 13 is the step response of Case 2 and its synchronous error $\overline{e}$ is shown as Fig. 14. $y_2$ lags behind $y_1$ in VCFM owing to coupled intensity and fixed supply pressure. However, in PCFM, responses of $y_1$ and $y_2$ are match with each other in the transient process, and it has better level control performance than VCFM. $\overline{e}$ of both VCFM and PCFM are increased as the coupled intensity increased but their difference are slightly. Again, rising time of $y_1$ and $y_2$ are 2.07 s and 2.10 s which are faster than those of PCFM. Nevertheless, the maximum over-

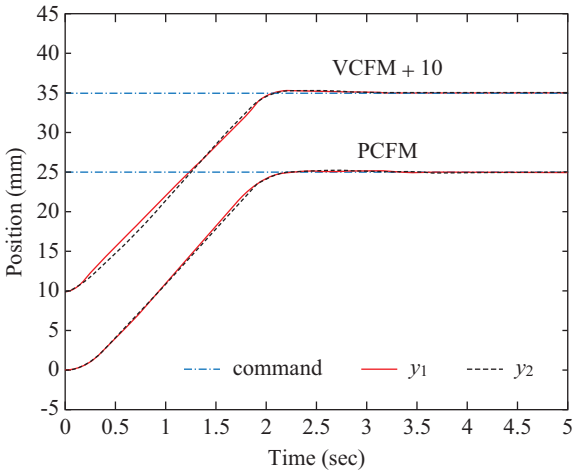


**Fig. 13. Step response of PCFM and VCFM of Case 2.**

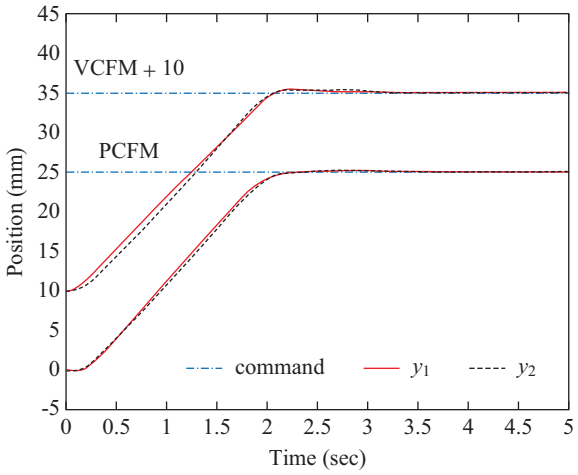


**Fig. 15. Step response of PCFM and VCFM of Case 3.**

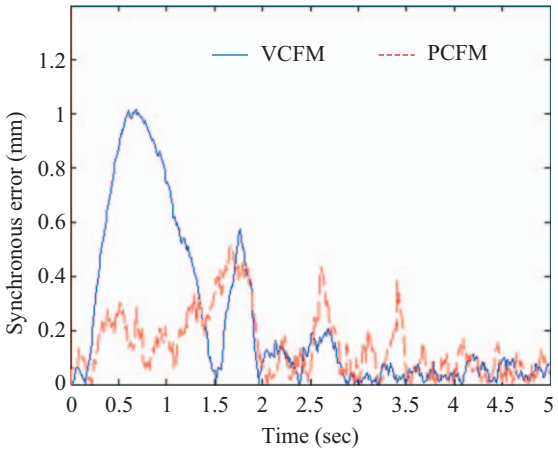


**Fig. 14. $\bar{e}$ of Case 2 of step command.**

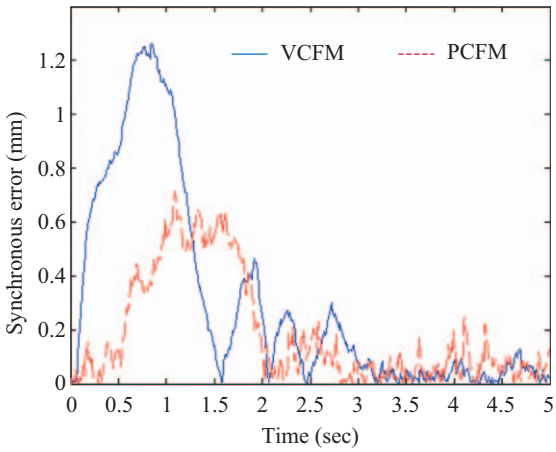


**Fig. 16. $\bar{e}$ of Case 3 of step command.**

shoot of $y_1$ and $y_2$ are 1.40% and 1.44% which are larger than those of PCFM. $\bar{e}_{av}$ of VCFM are 0.26 mm, which still higher than 0.16 mm of PCFM. $\bar{e}_{SS}$ of VCFM is 0.04 mm, which is still better than 0.06 mm of PCFM.

Fig. 15 is the step response of Case 3 and Fig. 16 is its synchronous error $\bar{e}$. Again, $\bar{e}$ of both VCFM and PCFM are increased due to high coupled intensity. Rising times of VCFM indicated in Table 2 are shorter than those of PCFM. However, its maximum overshoots are larger than those of PCFM. $\bar{e}_{av}$ of PCFM is 0.19 mm, which still has better synchronous performances than that of VCFM, $\bar{e}_{SS}$ of VCFM is 0.05 mm, which is still better than that of PCFM.

Owing to the disturbance of folding machine is spring force, the sliding mode control used in acceleration or force control will produce a slight overshot, especially at high speeds. In addition, inappropriate learning rate $\gamma$, adaptation gain $\delta_{ii}$ and coupled adaptation gain $\delta_{ij}$ will cause the system divergence and oscillation.

In comparison of Case 1~Case 3, $\bar{e}_{av}$ and $\bar{e}_{SS}$ are increased due to the increase of coupled intensity. In each case, rising time delay time and peak time of VCFM is shorter than those of PCFM as a result of higher supply pressure, which means VCFM has a faster response than PCFM. $\bar{e}_{av}$ of PCFM are lower than those of VCFM due to the variable supply pressure, it indicates that PCFM has a better synchronicity than those of VCFM. $\bar{e}_{SS}$ of VCFM are lower than those of PCFM, it indicates that VCFM has a better steady state performance than those of PCFM.

## VI. CONCLUSION

From previous efforts, following conclusions of VCFM and PCFM can be drawn:

1. Both VCFM and PCFM are coupled MIMO systems. The CASOSMFC controller can be designed for the level control function.

2. VCFM and PCFM are different systems, before comparison, it must set the same basis for VCFM and PCFM.
3. PCFM uses two groups of the power unit to drive two subsystems, the resistance of two subsystems is almost the same, theirs saturation voltage and proportional gain ratio KP of two axes are the same. VCFM uses a group of the power unit to drive two subsystems, the resistance of two subsystems is different, theirs saturation voltage and proportional gain ratio KP of two axes are different.
4. VCFM has higher supply pressure in the working process. Its transient response is faster than PCFM and cause larger maximum overshoot and it uses a group of the power unit to drive two subsystems, the resistance of two subsystems is different, cause larger $\overline{e}_{av}$, however, its $\overline{e}_{SS}$ is a little bit better than PCFM.
5. PCFM has variable working pressure and initial pressure is low, which degrade the rising time and it uses two groups of the power unit to drive two subsystems, the resistance of two subsystems is almost the same and got better $\overline{e}_{av}$, however, its $\overline{e}_{SS}$ is a little bit worse than VCFM.
6. Experimental results indicate that although the transient and steady state response of PCFM and VCFM are similar, and VCFM has a little bit better $\overline{e}_{SS}$ than PCFM, but PCFM has better $\overline{e}_{av}$ than VCFM. Thus, PCFM is an option to replace VCFM in the position synchronous level control applications.

## ACKNOWLEDGEMENTS

This work is funded by Ministry of Science and Technology of Taiwan, R.O.C. under the grant number MOST 104-2221-E-146-010-.

## REFERENCES

Chen, Z. (2015). Application of multi-objective controller to optimal tuning of PID gains for a hydraulic turbine regulating system using adaptive grid particle swam optimization. ISA Transactions 56, 173-187.

Cheng, G. and S. Pan (2008). Nonlinear adaptive robust control of single-rod electro-hydraulic actuator with unknown nonlinear Parameters. IEEE Trans. on Control Systems Tech. 16, 3, 434-445.

Chiang, M. H. (2011). A novel pitch control system for a wind turbine driven by a variable-speed pump-controlled hydraulic servo system. Mechatronics 21, 753-761.

Chiang, M. H, C. C. Chen and C. F. Kuo (2009). The high response and high efficiency velocity control of a hydraulic injection molding machine using a variable rotational speed electro-hydraulic pump-controlled system. International Journal of Advanced Manufacturing Technology 43, 9-10, 841-851.

Chiang, M. H. and Y. W. Chien (2003). Parallel control velocity control and energy-saving control for a hydraulic valve-controlled cylinder system using self-organizing fuzzy sliding model control. JSME International Journal, Series C: Mechanical Systems, Machine Elements and Manufacturing 46, 1, 224-231.

Jones, E., A. Dobson and A. P. Roskilly (2000). Design of a reduced-rule self-organizing fuzzy logic controller for water hydraulic applications. Proceedings of the Institution of Mechanical Engineers. Part I, Journal of systems and control engineering 214, 5, 371-381.

Kim, G. W. and K. W. Wang (2009). Switching sliding mode force tracking control of piezoelectric-hydraulic pump-based friction element actuation systems for automotive transmissions. Smart Materials and Structures 18, 8, 1-15.

Lin, J. and R. J. Lian (2008). DSP-based self-organizing fuzzy controller for active suspension systems. Vehicle System Dynamics 46, 12, 1123-1139.

Maldonado, Y., O. Castillo and P. Melin, (2014). A multi-objective optimization of type-2 fuzzy control speed in FPGAs. Applied Soft Computing. Applied Soft Computing. 24, 1164-1174.

Mirkin, B. and P. Gutman (2015). Multivariable output feedback robust adaptive tracking control design for a class of delayed systems. International Journal of Systems Science 46, 3, 429-437.

Mohanty, A. and B. Yao (2011). Indirect adaptive robust control of hydraulic manipulators with accurate parameter estimates. IEEE Transactions on Control Systems Technology 19, 3, 567-575.

Tar, J. K., I. J. Rudas, A. Szeghegyi and K. Kozlowski (2005). Nonconventional processing of noisy signals in the adaptive control of hydraulic differential servo cylinders. IEEE Trans. on Instrumentation and Measurement 54, 6, 2169-2176.

Yang, C., Y. Li, S. S. Ge and T. H. Lee (2010). Adaptive control of a class of discrete-time MIMO nonlinear systems with uncertain couplings. International Journal of Control 83, 10, 2120-2133.

Yang, G., J. Yao, G. Le and D. Ma (2016). Adaptive integral robust control of hydraulic systems with asymptotic tracking. Mechatronics 40, 78-86.

Yuan, X., Z. Chen, Y., Yuan and Y. Huang (2015). Design of fuzzy sliding mode controller for hydraulic turbine regulating system via input state feedback linearization method. Energy 93, 173-187.

Zhang, J., X. Mei, D. Zhang, G. Jiang and Q. Liu (2012). Application of decoupling fuzzy sliding mode control with active disturbance rejection for MIMO magnetic levitation system. Proc. IMechE Part C:J Mechanical Engineering Science 227, 2, 213-229.